Cathode Materials

DOI: 10.1002/anie.200701473

On the Structure of Carbon-Supported Selenium-Modified Ruthenium Nanoparticles as Electrocatalysts for Oxygen Reduction in Fuel Cells**

*Gerald Zehl, Gerrit Schmithals, Armin Hoell, Sylvio Haas, Christoph Hartnig, Iris Dorbandt, Peter Bogdanoff, and Sebastian Fiechter**

Dedicated to Süd-Chemie on the occasion of its 150th anniversary

Currently, platinum-based catalysts are state-of-the-art materials for the oxygen reduction reaction (ORR) in low-temperature fuel cells. The use of Pt nanoparticles finely dispersed on supports with extremely large surface areas led to a remarkable reduction of the required amount of Pt.[1] However, the applicability of fuel cells is still bound to this rare and expensive metal. Therefore, numerous research groups have evaluated the substitution of Pt by Ru as a catalytically less active but cheaper and more consistently available alternative.[2–4] Alonso-Vante et al. discovered that the activity of Ru-based catalysts can be significantly enhanced by selenium.[5] Moreover, Se-modified materials also feature superior methanol tolerance. Therefore, these catalysts are of particular interest for direct methanol fuel cells (DMFCs), in which undesired methanol crossover into the cathode compartment is an unsolved problem. Although intensive studies on $RuSe_x$ catalysts were performed, no definite conclusion regarding the nature of the catalytically active surface and the constitution of the $RuSe_x$ nanoparticles could be drawn.[6–9] However, this information is believed to be the prerequisite for further catalyst optimization.

Previously, $RuSe_x$/C catalysts were prepared from Ru carbonyl precursor compounds. $[Ru_3(CO)_{12}]$ was decomposed in Se-saturated xylene in the presence of carbon black at 140 °C.[10] In this process, Ru particles are formed in solution, and the Se modification occurs by precipitation of elemental Se during cooling of the reaction mixture. The nonuniform distribution of the $RuSe_x$ particles on the support and the poor controllability of the extent of their Se modification were identified as main disadvantages of this technique.[11]

Currently, $RuSe_x$/C catalysts are prepared in a multistep procedure starting from ionic metal precursors. Carbon-supported Ru nanoparticles are obtained from aqueous solution of $RuCl_3 \cdot x\,H_2O$ containing suspended carbon black. After homogenization of the mixture using ultrasound, the solvent is removed, and the dried catalyst is reductively treated at 200 °C. This Ru/C intermediate is then transferred to an acetone solution of $SeCl_4$, and the solvent is removed. The Se content of the resulting dried powders varies depending on the amount of $SeCl_4$ employed.[12] A final reductive treatment, typically at 300 °C, activates the catalyst.

The electrochemical activity of the catalysts was characterized by the limiting kinetic current j_k from rotating disc electrode (RDE) measurements at $U = 0.7$ V versus the standard hydrogen electrode. Since ORR proceeds on the surface of the $RuSe_x$ nanoparticles, RDE current should be sensitive to the amount of Se modifying their surface. Indeed, optimum Se content was found at about 7 wt % on a sample with about 40 wt % Ru, which corresponds to the maximum of curve a in Figure 1. The weaker activity at higher loadings can

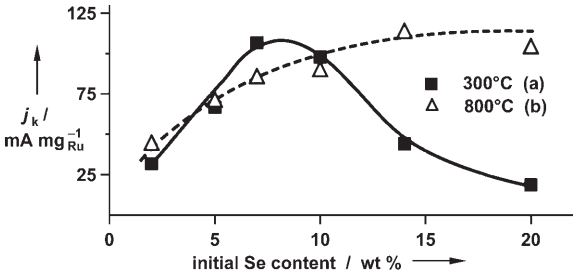

Figure 1. Influence of the initial Se content of a Ru–Se/C catalyst (40 wt % Ru) on their ORR activity. The reductive treatment temperatures during Se modification were 300 °C (a) and 800 °C (b). CO_2-activated "Black Pearls 2000" from Cabot Corp. were used as the carbon support.

be explained by increased blocking of active sites with excess Se. However, surplus Se can be easily removed by reductive annealing at temperatures up to 800 °C.[12] Although Se forms many volatile species even below its boiling point at 690 °C, higher temperatures are required for a complete removal of loosely interacting Se. Accordingly, annealing under forming gas ($N_2/H_2 = 95:5$) at 800 °C was found to remove excess Se reliably while preserving the strong Ru–Se interaction.[12] Correspondingly, curve b in Figure 1 shows a high activity for samples with initially high Se content. On the other hand,

[*] Dr. G. Zehl, Dr. G. Schmithals, Dipl.-Ing. I. Dorbandt, Dr. P. Bogdanoff, Dr. S. Fiechter
Department of Solar Energetics SE-5
Hahn-Meitner-Institute Berlin
Glienicker Strasse 100, 14109 Berlin (Germany)
Fax: (+49) 30-8062-2434
E-mail: fiechter@hmi.de
Dr. A. Hoell, Dipl.-Phys. S. Haas
Department of Structural Research SF-3
Hahn-Meitner-Institute Berlin
Glienicker Strasse 100, 14109 Berlin (Germany)
Dr. C. Hartnig
Zentrum für Solarenergie- und Wasserstoff-Forschung ZSW
Helmholtzstraße 8, 89081 Ulm (Germany)

[**] We gratefully acknowledge financial support from BMBF under grant no. 03SF0302, and we thank Dr. D. Alber for NAA analysis of the catalysts.

$RuSe_2$ (the only described stoichiometric RuSe compound) is thermally stable only up to 950 °C.[13] Therefore, when annealing the samples, this temperature must not be exceeded.[12]

To quantify the Se loss during annealing, the Se/Ru mass ratio of all catalysts was determined via neutron activation analysis (NAA). The Se/Ru ratio follows the initial amount of Se introduced as $SeCl_4$ when the annealing temperature is low (Figure 2a). At 800 °C, the ratio levels off at Se/Ru ≈ 0.3, even when preparation started with higher initial amounts of Se (Figure 2b). As shown previously, Se also interacts with the carbon support at ambient conditions. Therefore, Se/Ru ratios determined from samples treated at 300 °C do not allow conclusions about the extent of Se modification of the Ru nanoparticles. However, after annealing at 800 °C, the interaction of Se with carbon can be neglected.[12] Hence, determination of the metal content of catalysts thus annealed affords the average Se/Ru ratio within the supported $RuSe_x$ nanoparticles. Therefore, the plateau in curve b indicates an upper limit of the achievable extent of Se modification of the Ru nanoparticles.

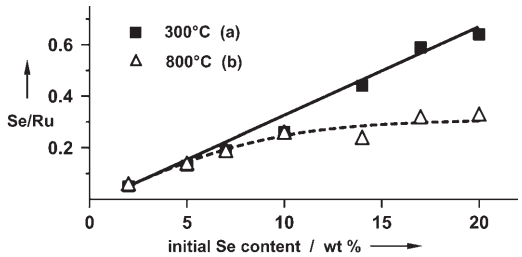

Figure 2. Influence of the annealing temperature and the initial Se content on the average Se/Ru mass ratio of the final catalysts.

To deduce an applicable structural model of these particles, a $RuSe_x$ catalyst with 40 wt% Ru and 14 wt% Se reductively annealed at 800 °C was characterized in detail. TEM images suggest the existence of dense nanoparticles of approximately 2.5 nm in size, uniformly distributed over the less dense carbon support (Figure 3a). From XRD, an average Ru particle size of 2.2 nm can be deduced. The XRD trace of the catalyst does not show any crystalline phases except hcp Ru (Figure 3b).

As shown earlier, thermal treatment of Ru-free Se/C material at 800 °C virtually eliminates all Se–C interactions, leaving behind Se-free carbon black.[12] On the other hand, when tempering $RuSe_x$/C likewise Se remains on the catalysts (Figure 2, curve b) but no other phases than hcp Ru (Figure 3b) are formed. Therefore, we hypothesize a structural model assuming firmly interacting Se that only partially decorates the surface of primary Ru core particles.[13]

This assumption is also supported by structural considerations: 2.5-nm hcp Ru particles consist of about 580 atoms. Around 275 of these atoms (45% of the total) belong to the surface, that is, they are coordinated by less than 12 neighbors. As derived from curve b in Figure 2, the limiting Se/Ru mass ratio of our catalysts is 0.3, which corresponds to a Se/Ru molar ratio of 0.38. Therefore, presuming that one Ru surface atom provides at least one bonding site for Se (which is a lower limit), the available amount of Se is actually insufficient even to form a Se monolayer that could cover the whole Ru surface.

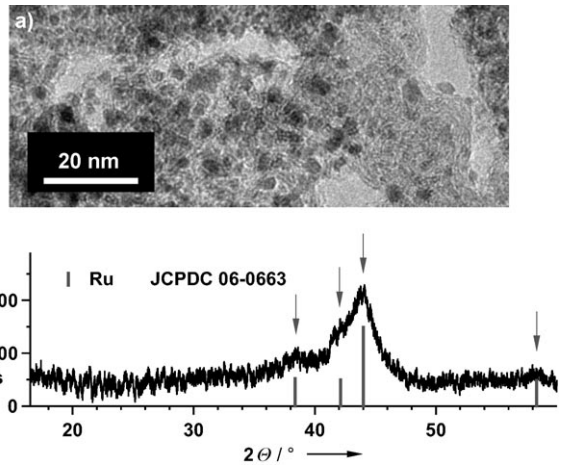

Figure 3. TEM image (a) and XRD spectrum (b) of the Ru–Se/C catalyst (40 wt% Ru) used for ASAXS measurements. The catalyst was reductively annealed at 800 °C before characterization. CO_2-activated "Black Pearls 2000" from Cabot Corp. were used as the carbon support.

To elucidate the distribution of Se atoms on the surface of the Ru particles, anomalous small-angle X-ray scattering (ASAXS) experiments were performed. ASAXS takes advantage of the so-called anomalous or resonant behavior of the atomic scattering amplitude of an element near its absorption edge to separate its scattering contribution from other elements in the sample.[14,15]

A set of samples was studied, including the final $RuSe_x$/C catalyst, intermediate preparation states such as Se-free Ru nanoparticles, and the bare CO_2-treated carbon support. The scattering curves were taken at five energies where the anomalous scattering amplitude f' varies nearly equidistant in the vicinity below the Se and the Ru K absorption edges. Special care was taken to extend the q range to larger values to obtain structural information from sub-nanometer structures.

Figure 4a shows nanostructures formed by Ru and Se that alter the shape of the carbon support's ("Black Pearls") scattering curve dramatically. Two significant shoulders at $q = 1\ nm^{-1}$ and $q = 7\ nm^{-1}$ are detected. A clear anomalous scattering effect at the Ru edge (inset in Figure 4a) identifies Ru-containing structures. In addition, it was deduced that Se within the sample generates clearly detectable sub-nanometer-sized structural features.

Taking into account the energy dependences (the anomalous dispersion effect) of the scattering intensity at both absorption edges, a structural model of the catalytically active nanoparticles has been deduced. This model suggests nearly spherical Ru particles with a mean diameter of 2.5 nm decorated with Se-containing clusters with a diameter less than 0.6 nm. These clusters could exhibit symmetric, ring-like structures as observed for free Se.[16]

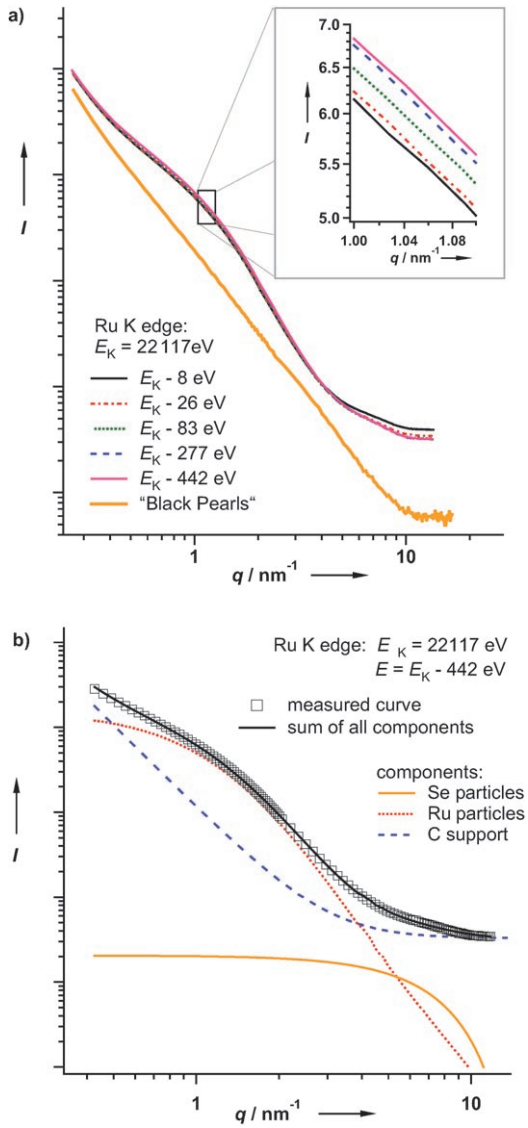

Figure 4. ASAXS curves (a, logarithmic) show a clear resonant behavior (inset) of the RuSe catalyst at the Ru K edge in comparison with pure "Black Pearls". Three structural elements could be identified (b). Their sum models the measured scattering intensities.

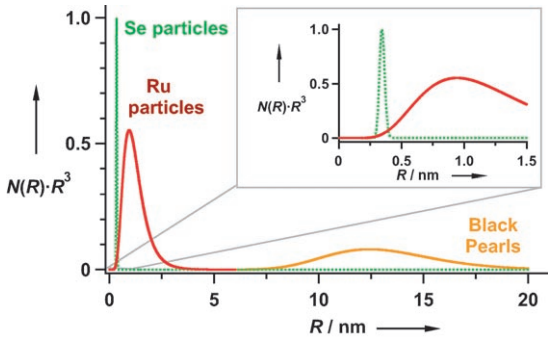

Figure 5. Volume-weighted size distributions of three structural components.

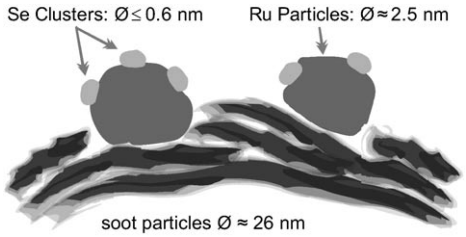

Figure 6. Suggested structural model derived from ASAXS and SANS (small-angle neutron scattering).

Figure 4b shows the partial scattering intensities of all three identified structural components. Their sum fits the measured curve very well. This summation holds for all X-ray energies. Figure 5 shows the volume-weighted size distributions of the structural components. The simplified picture in Figure 6 illustrates the morphology of the catalyst.

To gain further insight into structure and bonding of the $RuSe_x$ particles, the same material was subjected to EXAFS (extended X-ray absorption fine structure) analysis at the Ru and Se K edges. At the Ru K edge, the Fourier transformed EXAFS function (R–χ space) exhibits two main structural features: a dominant broad peak at $R = 1.45$ Å and a sharp peak at $R = 2.3$ Å (Figure 7a). The first feature is related to Ru–O bonds as known from RuO_2 and the latter to Ru–Ru bonds found in hcp Ru. This assignment becomes evident from the coincidence of the hcp Ru reference curve with the FT-EXAFS spectrum of the investigated catalyst at higher R values. It indicates that longer Ru–Ru distances are also present in the $RuSe_x$ particles, thus demonstrating that their core consists of metallic Ru. No congruence at higher R values was found between the RuO_2 reference and the FT-EXAFS spectrum of the catalyst, pointing to a reaction of oxygen only with Ru surface atoms, for example, during the exposure of the catalyst to air.

Se–Ru bonds can be detected at the Se K edge (Figure 7b). As expected, the main feature of the catalyst's FT-EXAFS curve coincides with the main peak of the $RuSe_2$ reference, thus indicating Ru–Se bonds of the same distance as in $RuSe_2$. However, the absence of further peaks at higher R values again indicates that Se–Ru bonds must be restricted to the surface of the Ru particles and that no $RuSe_2$ phase has been formed. Therefore, the observed curve is close to a simulated Ru–Se scattering curve considering only the smallest Se–Ru distance. The differences between the simulated and measured curves can be attributed to partial oxidation of selenium (Se–O bonds) and to Se–Se bonds on the surface of the catalyst particles. By careful fitting of the curve measured at the Se K edge, a coordination number $N < 4$ for Se could be inferred, which again indicates bonding of Se at the surface. In conclusion, the Se-modified Ru particles can be considered as $RuSe_xO_y$ assuming covalent bonding of oxygen and Se as found in oxyselenides.

We have shown that Se-modified Ru nanoparticles on $RuSe_x$/C catalysts are not completely covered by Se on the particle surface after reductive annealing at 800 °C. The Se forms clusters on the Ru surface while the rest of the surface is

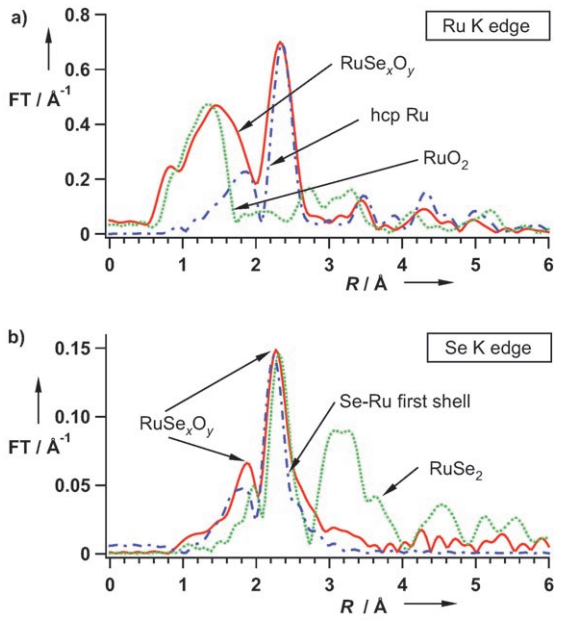

Figure 7. FT-EXAFS spectra of the RuSe$_x$ catalyst annealed at 800 °C with the reference curves measured a) at the Ru K edge, and b) at the Se K edge.

covered by oxygen. This type of catalyst has proven highly active in the ORR at the cathode side in DMFC.

Experimental Section

RDE measurements were performed in a one-compartment glass cell at room temperature in 0.5 M H_2SO_4. The catalyst was attached to a working electrode consisting of a PTFE-surrounded glassy carbon rod ($\varnothing = 3$ mm, PTFE = polytetrafluoroethylene). A mercury sulfate electrode served as the reference and a Pt wire as the counter electrode. The kinetic current was calculated using the Koutecky–Levich equation.[11,17] The RDE was prepared as follows: Catalyst (1 mg) was suspended in a 0.2 % Nafion solution (200 μL). A portion of this suspension (5 μL) was then transferred onto the GC electrode and dried in air at 60 °C.

XRD measurements were recorded on a SIEMENS D500 ($Cu_{K\alpha}$, $\lambda = 0.154178$ nm) diffractometer. TEM images were taken using a Philips CM 12 electron microscope at 120 kV.

EXAFS was performed at Hasylab (Hamburg) at beamlines X and C employing a double crystal monochromator. Experiments were done at room temperature in standard geometry allowing parallel measurements of transmission and fluorescence signals. The analysis was performed using the ab initio multiple scattering algorithm FEFF.

ASAXS was performed at 7T-MPW-SAXS at the synchrotron facility BESSY in Berlin. For the simulations a spherical particle model and a log-normal distribution were assumed. The upper error limit in size determination of the Se structures amounts to 20 %.

Received: April 5, 2007
Revised: June 5, 2007
Published online: September 4, 2007

Keywords: fuel cells · heterogeneous catalysis · ruthenium · selenium · X-ray scattering

[1] S. Srinivasan, E. A. Ticianelli, C. R. Derouin, A. Redondo, *J. Power Sources* **1988**, *22*, 359.
[2] N. Alonso-Vante, H. Tributsch, O. Solorza-Feria, *Electrochim. Acta* **1995**, *40*, 567.
[3] V. Trapp, P. Christensen, A. Hamnett, *J. Chem. Soc. Faraday Trans.* **1996**, *92*, 4311.
[4] F. R. Rodríguez, P. J. Sebastian, O. Solorza, R. Pérez, *Int. J. Hydrogen Energy* **1998**, *23*, 1031.
[5] N. Alonso-Vante, P. Bogdanoff, H. Tributsch, *J. Catal.* **2000**, *190*, 240.
[6] N. Alonso-Vante, *Fuel Cells* **2006**, *6*, 182.
[7] N. Alonso-Vante, I. V. Malakhov, S. G. Nikitenko, E. R. Savinova, D. I. Kochubey, *Electrochim. Acta* **2002**, *47*, 3807.
[8] D. Cao, A. Wieckowski, J. Inukai, N. Alonso-Vante, *J. Electrochem. Soc.* **2006**, *153*, A869.
[9] V. I. Zaikovskii, K. S. Nagabhushana, V. V. Kriventsov, K. N. Loponov, S. V. Cherepanova, R. I. Kvon, H. Bönnemann, D. I. Kochubey, E. R. Savinova, *J. Phys. Chem. B* **2006**, *110*, 6881.
[10] O. Solorza-Feria, K. Ellmer, M. Giersig, N. Alonso-Vante, *Electrochim. Acta* **1994**, *39*, 1647.
[11] M. Hilgendorff, K. Diesner, H. Schulenburg, P. Bogdanoff, M. Bron, S. Fiechter, *J. New Mater. Electrochem. Syst.* **2002**, *5*, 71.
[12] G. Zehl, I. Dorbandt, G. Schmithals, J. Radnik, K. Wippermann, B. Richter, P. Bogdanoff, S. Fiechter, *ECS Trans.* **2006**, *3*, 1261.
[13] S. Fiechter, I. Dorbandt, P. Bogdanoff, G. Zehl, H. Schulenburg, H. Tributsch, M. Bron, J. Radnik, M. Fieber-Erdmann, *J. Phys. Chem. C* **2007**, *111*, 477.
[14] G. Goerigk, H.-G. Haubold, O. Lyon, J.-P. Simon, *J. Appl. Crystallogr.* **2003**, *36*, 425.
[15] A. Hoell, F. Bley, A. Wiedenmann, J. P. Simon, A. Mazuelas, P. Boesecke, *Scr. Mater.* **2001**, *44*, 2335.
[16] J. Becker, K. Rademann, F. Hensel, *Z. Phys. D* **1991**, *19*, 229.
[17] M. Bron, P. Bogdanoff, S. Fiechter, M. Hilgendorff, J. Radnik, I. Dorbandt, H. Schulenburg, H. Tributsch, *J. Electroanal. Chem.* **2001**, *517*, 85.

